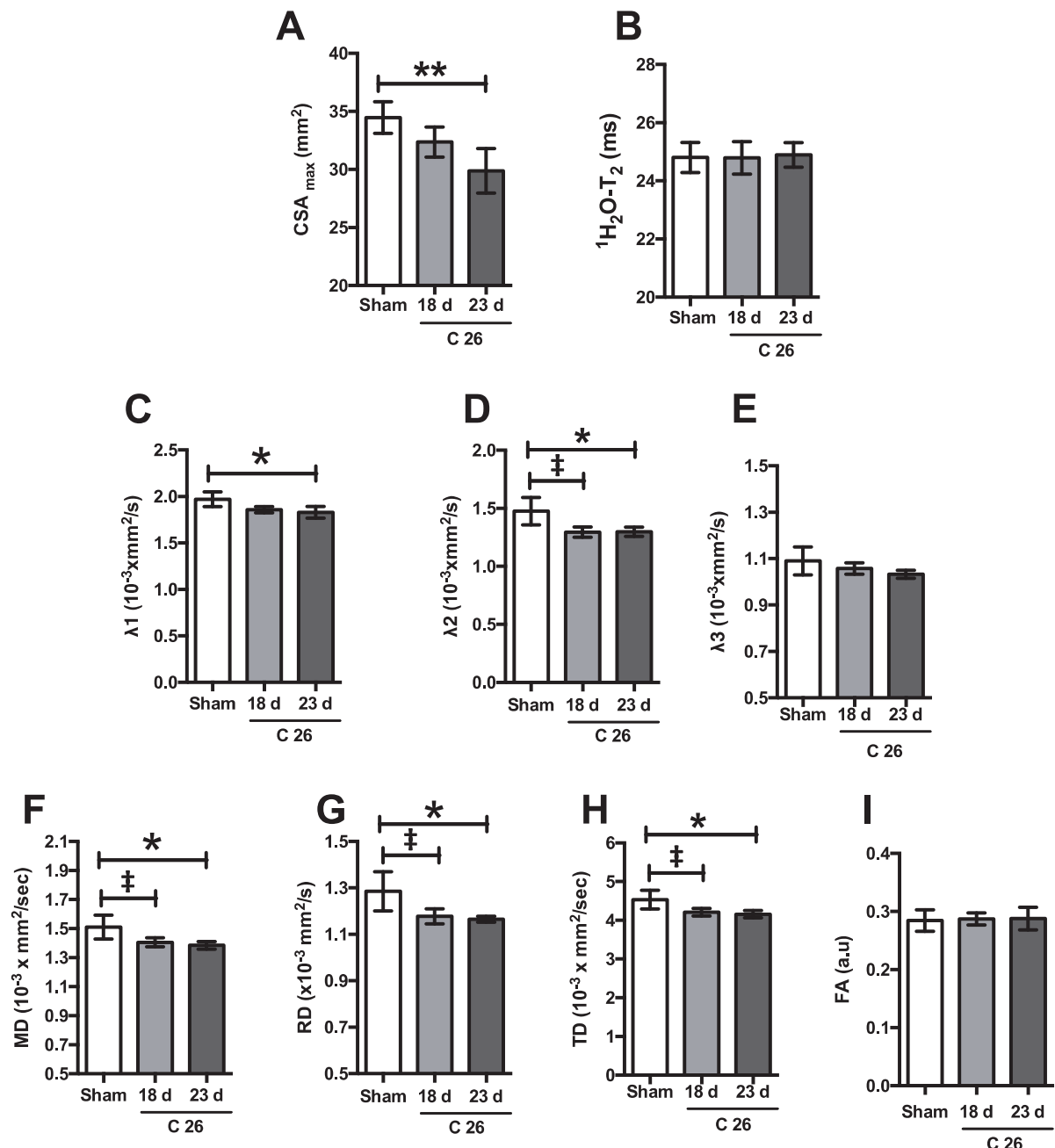


Supplemental Figures

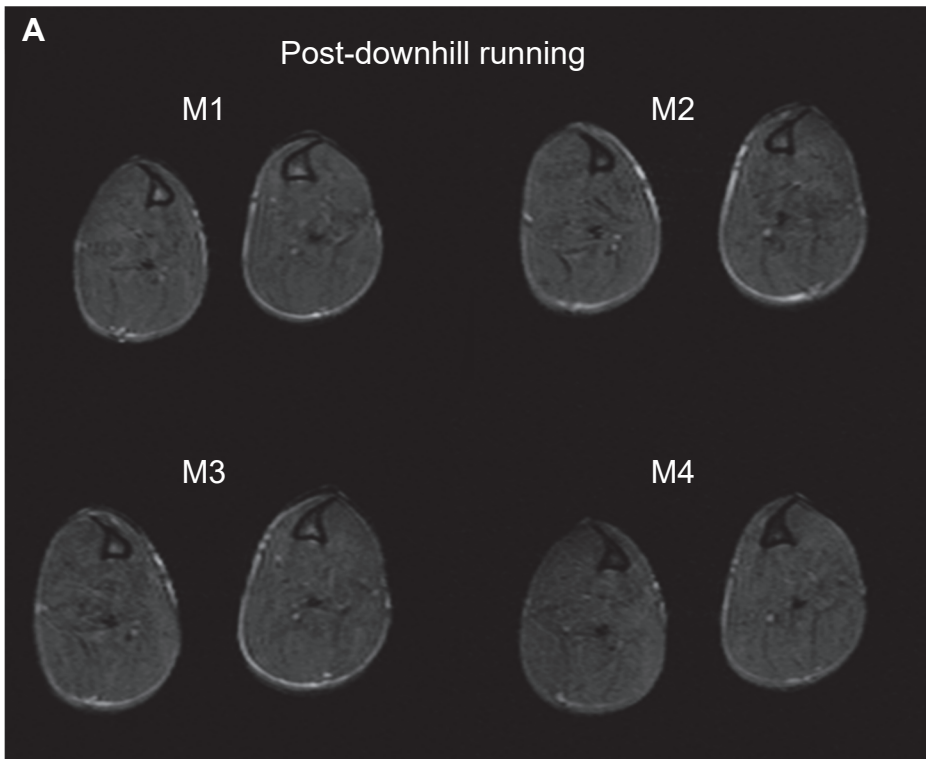
Judge et al. *Loss of Myoc via Mef2c mediates cancer cachexia*



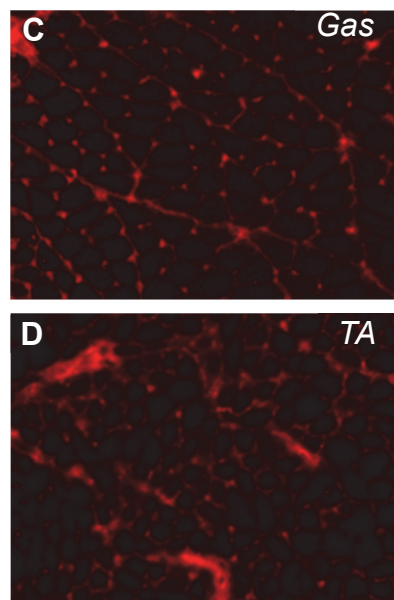
Supplementary Fig. S1. Diffusion tensor magnetic resonance imaging of lower hindlimb muscles of cage-restricted Sham and C26 tumor-bearing mice. Muscle cross sectional area (CSA_{\max}) (A) and MRS determined water T₂ (${}^1\text{H}_2\text{O-T}_2$) values (B) within posterior hindlimb muscles of sham and C26 tumor-bearing mice at day 18 and day 23 post tumor-cell inoculation. Eigenvalues ($\lambda_1, \lambda_2, \lambda_3$) (C-E), mean diffusivity (MD) (F), radial diffusivity (RD) (G), total diffusivity (TD) (H), and fractional anisotropy (FA) (I) determined within a region of interest in posterior (GAS-SOL complex) compartment muscles. MD, RD and TD were calculated using $(\lambda_1 + \lambda_2 + \lambda_3/3)$, $(\lambda_2 + \lambda_3/2)$, and $(\lambda_1 + \lambda_2 + \lambda_3)$ respectively. ‡ Represents significant difference between sham and C26 mice 18 days post tumor cell inoculation. * Represents significant difference between sham and C26 mice 23 days post tumor cell inoculation. In summary, significant differences were detected in the CSA_{\max} and in diffusion parameters of posterior compartment muscles between sham and moderately

cachectic C26 tumor-bearing mice, confirming muscle atrophy. However, muscle damage was not evident in C26 tumor-bearing (or Sham) mice based on MRS-determined water T₂ (¹H₂O-T₂) values.

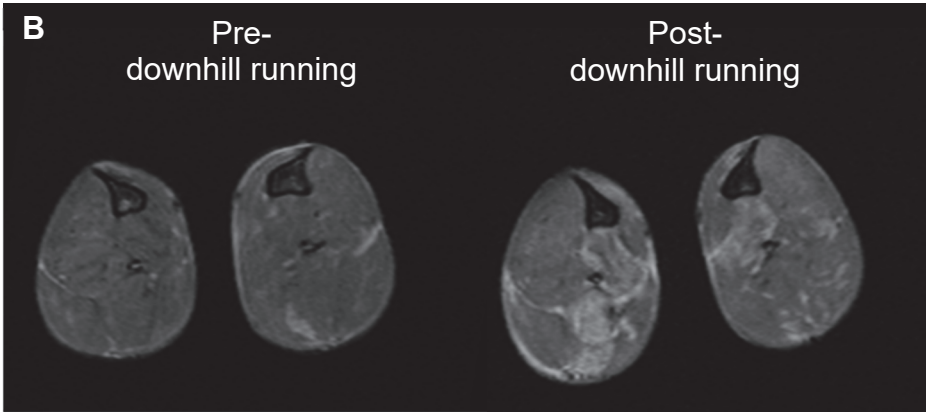
C26 tumor-bearing mice



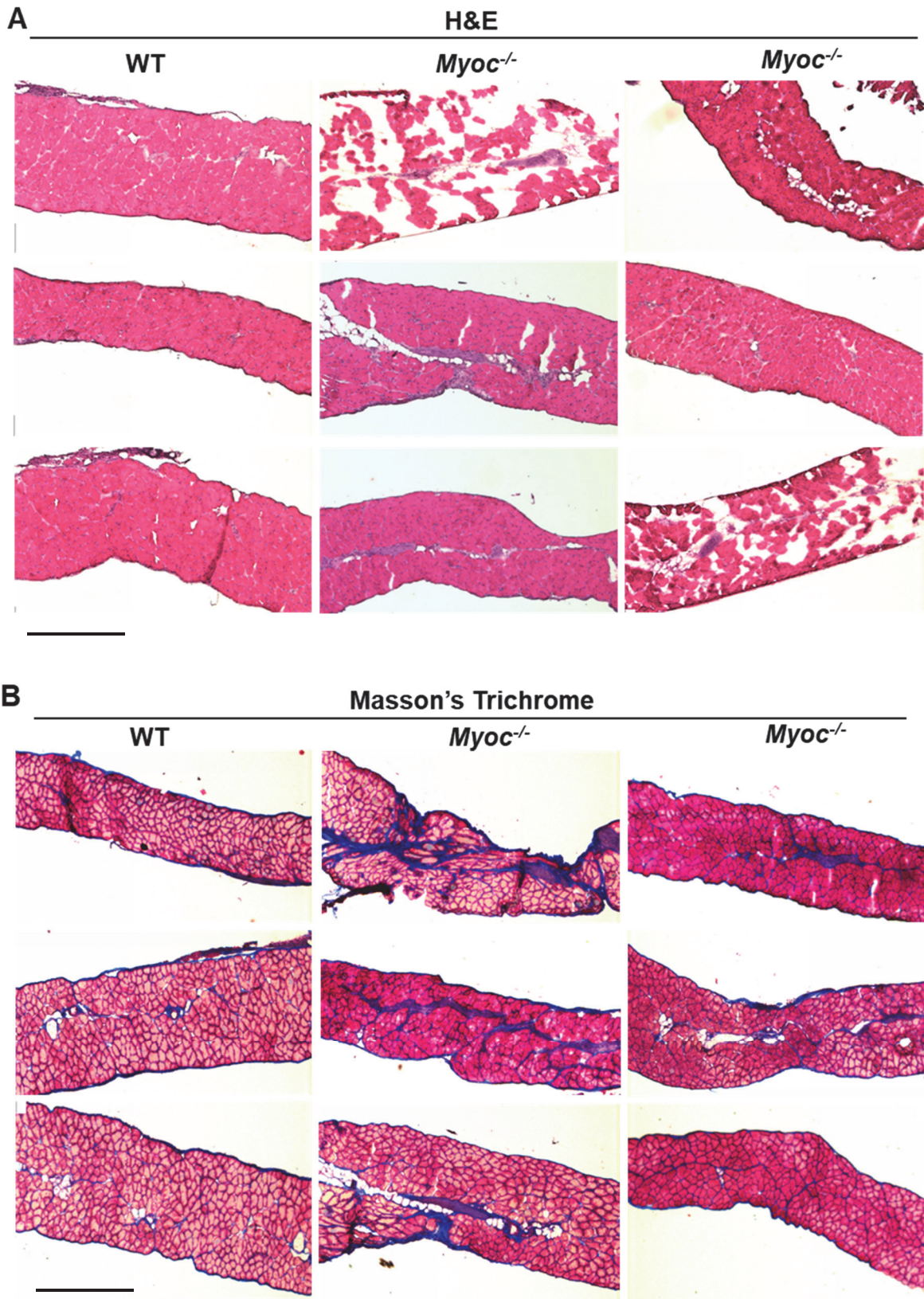
EBD



mdx (positive control)

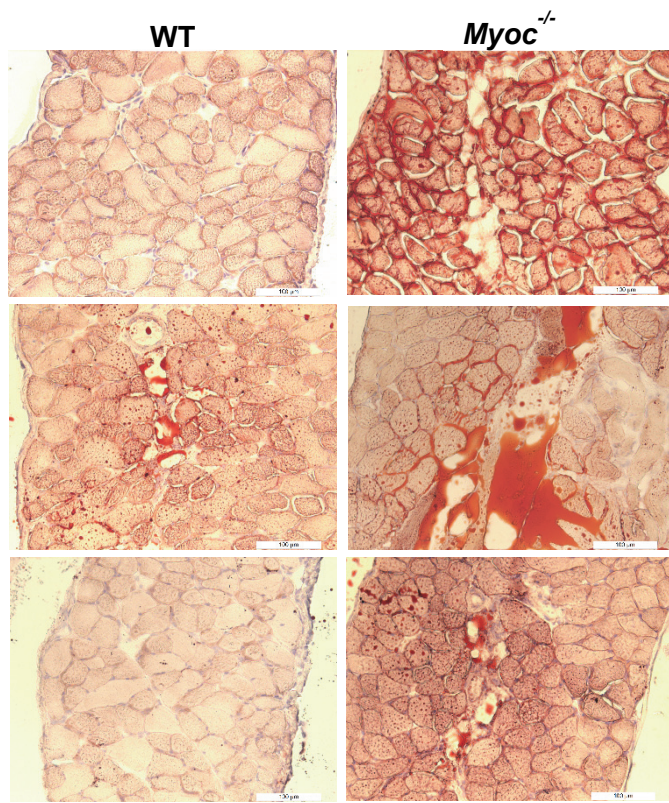


Supplemental Fig. S2. **A, B)** T2 weighted images captured via MRI from the lower hindlimbs of $n = 4$ cachectic C26 tumor-bearing mice (M1-M4) (**A**) and $n = 1$ *mdx* mouse (positive control, **B**) immediately following a single 45 min bout of treadmill running at a decline of 14°. This protocol induces significant muscle damage, as reflected by increased muscle T₂, in *mdx* mice, but not in C26 tumor-bearing mice, or control mice [data not shown and (6)]. **C, D)** Direct fluorescence imaging of Evan's Blue Dye (EBD) in sections from the gastrocnemius (**Gas**, **C**) and TA (**TA**, **D**) muscles from cachectic C26 tumor-bearing mice 1 day following downhill running. Myofiber uptake of EBD was not observed in the TA or the gas complex (soleus, plantaris or gas)—thus complementing the MRI data indicating lack of significant tearing of the sarcolemma in lower hindlimb muscles of cachectic C26 tumor-bearing mice following downhill running.

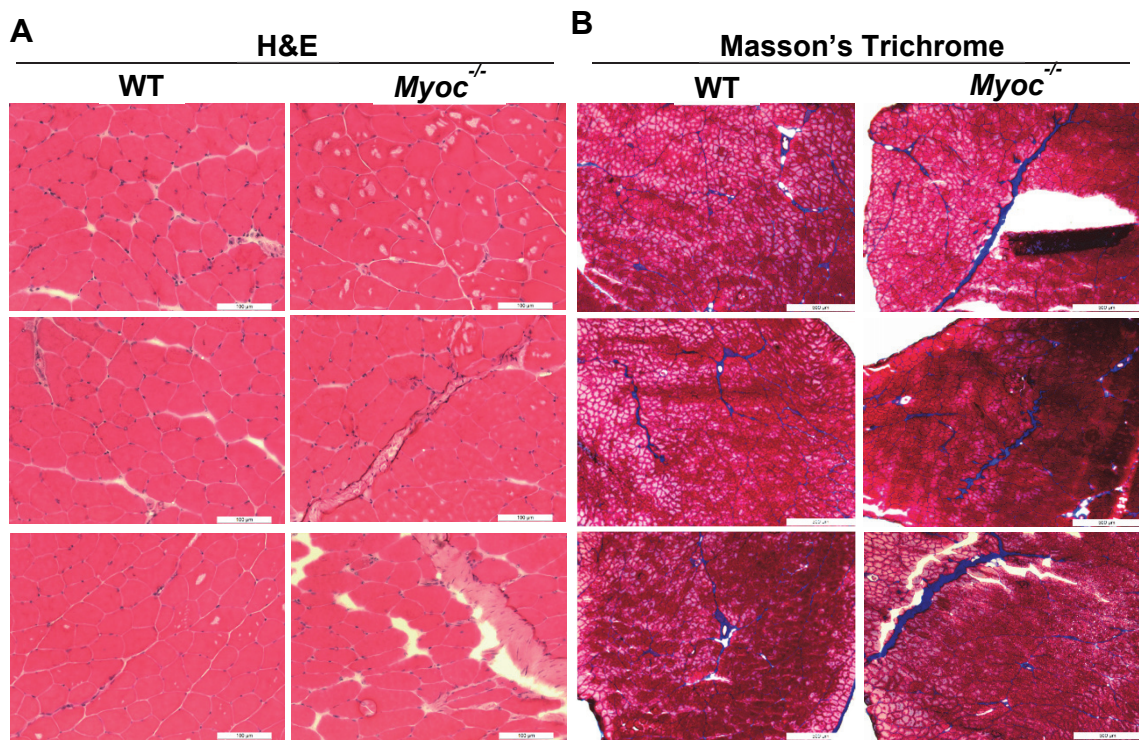


Supplemental Fig. S3. Diaphragm muscles of 18-month old *Myoc*^{-/-} mice show evidence of fibrosis. Representative cross-sections from diaphragm muscles of 18-month old WT and *Myoc*^{-/-} mice stained with H&E (A) or Masson's Trichrome (B), to label collagen (blue). Representative of n = 3 WT mice and n = 7 *Myoc*^{-/-} mice. Scale bars = 500 μ m.

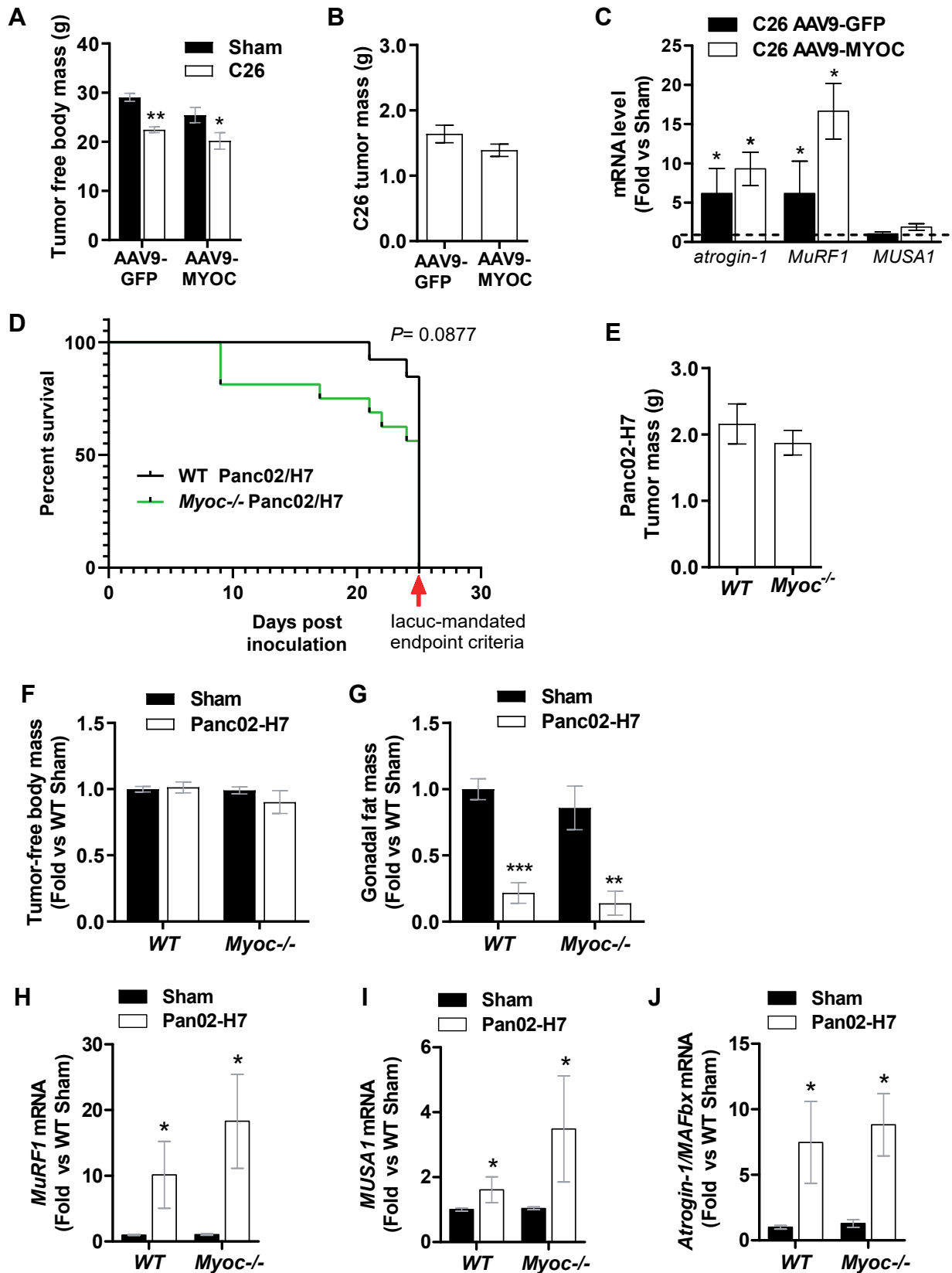
Oil Red O



Supplemental Fig S4. Diaphragm muscles of 18-month old *Myoc*^{-/-} mice show increased fat deposition. Representative cross-sections from the diaphragm of 18-month old WT and *Myoc*^{-/-} mice stained with Oil Red O to label fat (orange). Representative of n = 3 WT mice and n = 7 *Myoc*^{-/-} mice. Scale bars = 100 μ m.

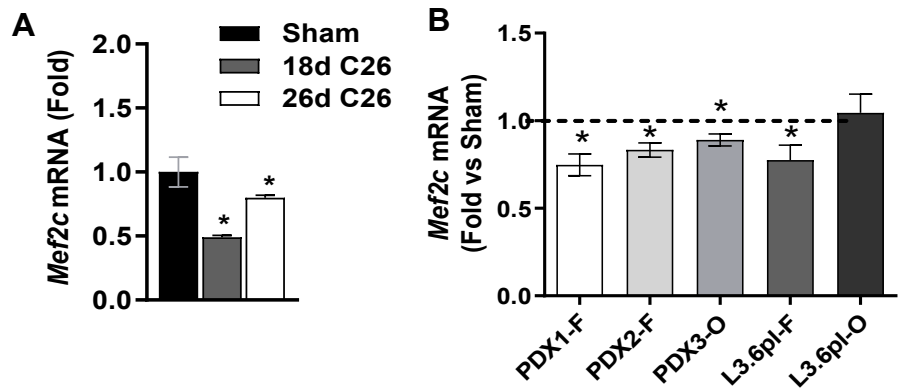


Supplemental Fig S5. TA muscles of 18-month old *Myoc*^{-/-} mice show evidence of fibrotic scarring. A,B) Representative cross-sections from the TA muscle of 18-month old WT and *Myoc*^{-/-} mice stained with H&E (A) or Masson's Trichrome (B) to label collagen (blue). Representative of n = 3 WT mice and n = 7 *Myoc*^{-/-} mice. Scale bar = 100 μ m (A), Scale bar = 500 μ m (B).

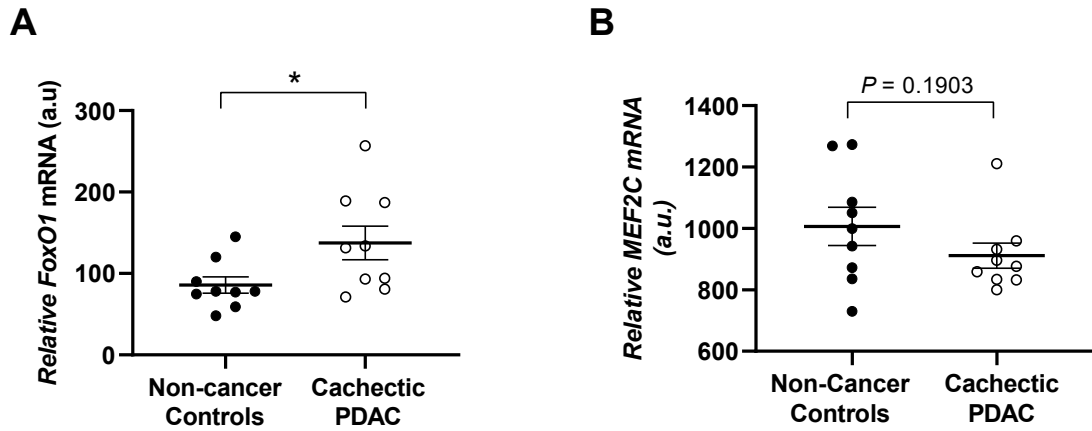


Supplemental Fig. S6. Tumor-free body mass (A) C26 tumor mass (B) and gene expression of atrophy genes (*atrogin-1*, *MuRF1*, *MUSA1*) in TA muscles (C) from sham and C26 tumor-bearing mice at tumor endpoint. Mice received either AAV9-GFP or AAV9-tMCK-MYOC-GFP injections into the TA 2 weeks prior to C26 tumor cell inoculations (* $P<0.05$, ** $P<0.01$, vs. respective sham group). Gene expression of *atrogin-1/Fbxo32*, *MuRF1/Trim63* and *MUSA1/Fbxo30* were normalized to

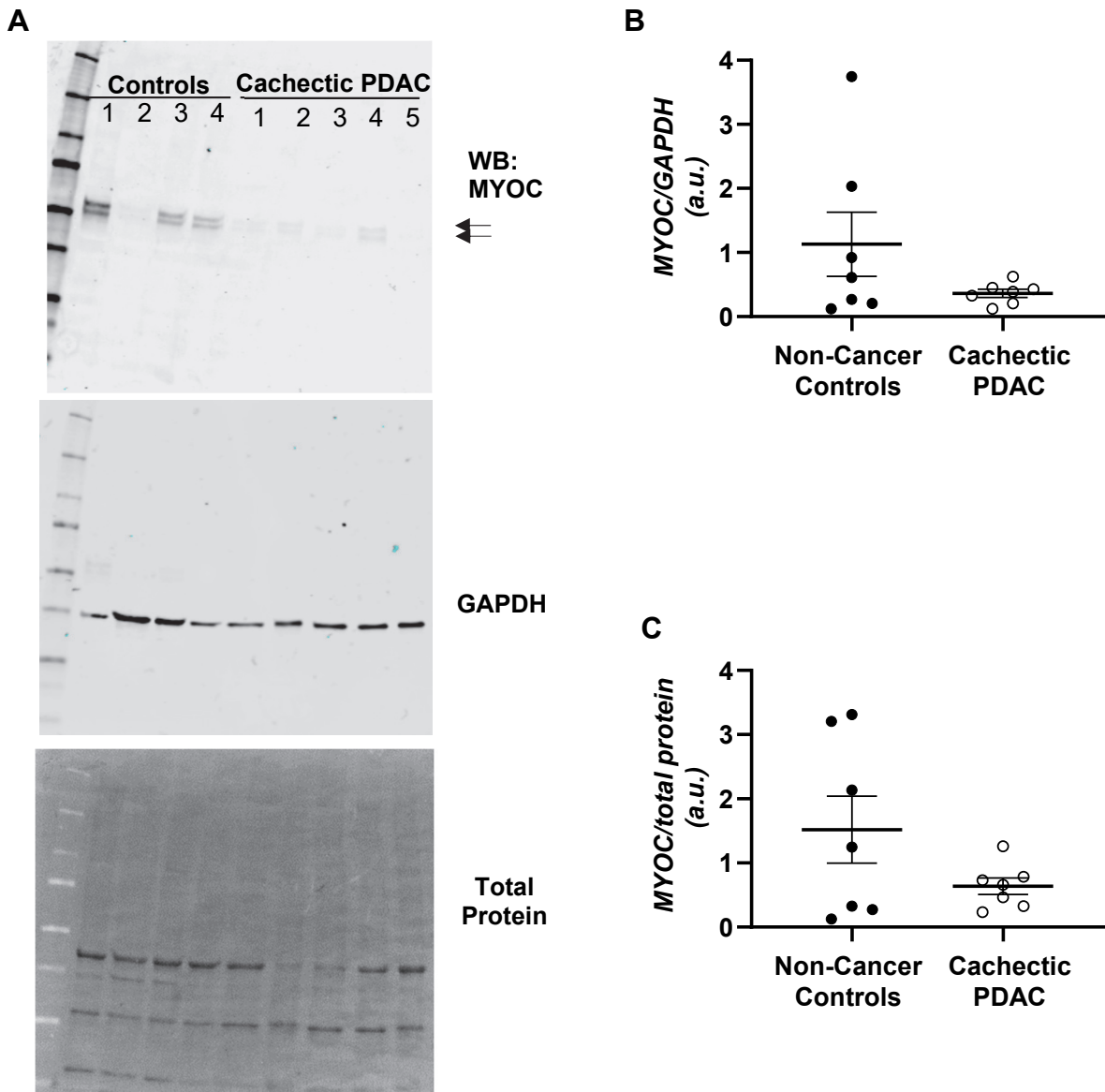
the respective sham group. **D**) Kaplan Meier curves generated from WT and *Myoc*^{-/-} mice bearing orthotopic Panc02/Panc02-H7 tumors. Survival time for each mouse strain bearing Panc02/Panc02-H7 tumors (data combined for tumor lines) was calculated based on dates of unanticipated deaths, or from the date in which IACUC-mandated experimental endpoints were reached, based on deterioration of body condition scores [Log-rank (Mantel-Cox) test; P = 0.0877; n = 13-16 tumor-bearing mice/group]. Tumor mass of orthotopic Panc02-H7 tumors (**E**), tumor-free body mass (**F**) and gonadal fat mass (**G**) from sham and/or tumor-bearing WT and *Myoc*^{-/-} mice at experimental endpoint. **H-J**) Gene expression of atrophy-related genes MuRF1/*Trim63* (**H**), MUSA1/*Fbxo30* (**I**) and atrogin-1/*Fbxo32* (**J**) within TA muscles from Sham and Panc02-H7 tumor-bearing WT and *Myoc*^{-/-} harvested at experimental endpoint. Gene expression was normalized to the WT sham group. *P<0.05 vs respective Sham group.



Supplemental Fig. S7. *Mef2c* is transcriptionally downregulated in skeletal muscle in multiple experimental models of cancer cachexia. **A)** Skeletal muscles harvested from C26 tumor-bearing mice were assessed for *Mef2c* mRNA on day 18 and day 26 post C26 tumor cell inoculation, which correspond to the early and more advanced stages of C26-induced muscle wasting, respectively (* $P<0.05$ vs Sham; n = 3-6 mice/group). **B)** The relative expression of *Mef2c* mRNA (vs Sham controls) was assessed in TA muscles in multiple experimental models of cancer cachexia, including in mice bearing human patient-derived xenograft (PDX) tumors implanted subcutaneously into the flank (PDX1-F, PDX2-F) or orthotopically into the pancreas (PDX-O), and in mice inoculated with human L3.6pl tumor cells subcutaneously into the flank (L3.6pl-F) or orthotopically into the pancreas (L3.6pl-O). Data are expressed as mean \pm SEM, normalized to that of mice receiving the respective sham surgery for each group (* $P<0.05$ vs Sham; n=4-6 mice/group).



Supplemental Fig. S8. A,B) Normalized levels of *FOXO1* mRNA (A) and *MEF2c* mRNA (B) in skeletal muscle biopsies from non-cancer controls with normal muscularity, compared to cachectic PDAC patients. Cachexia was defined based on body-weight loss of >8%, in combination with CT-defined measurements of muscle depletion and low muscle attenuation (MA)—cachexia thresholds which have been identified previously in cancer patients to associate with short survival (Martin et al., 2013).



Supplemental Fig. S9. MYOC protein expression in rectus abdominis muscle biopsies from non-cancer controls and cachectic PDAC patients. A-C) Equal amounts of skeletal muscle protein homogenate (from rectus abdominis muscle) from female non-cancer control patients and cachectic PDAC patients were probed for MYOC protein expression and normalized to either GAPDH expression (endogenous control) or total protein. A) Representative blots showing relative protein levels of MYOC and GAPDH, and total protein. B,C) Quantification of MYOC protein expression normalized to GAPDH (B) or total protein (C). PDAC patients were defined as cachectic based on body-weight loss of >8% in combination with CT-defined measures of muscle depletion based on low skeletal muscle index (SMI), and low muscle attenuation (MA), which have been previously established as cachexia thresholds that associate with short survival in cancer patients (Martin et al., 2013).